Natural Resources for Human Health

eISSN: 2583-1194

Original Research

Received 22 May 2026
Revised 26 June 2026
Accepted 22 July 2026

Natural Resources for Human Health 2026, Vol. 6 (8s): 997–1009

KEYWORDS:
HER2-ECD; human serum; electrochemical immunosensor; method comparison; ELISA; trastuzumab; pertuzumab; Bland–Altman analysis

Paired Human-Serum Evaluation of HER2 Immunosensors: Effects of Electrode Architecture and Trastuzumab/Pertuzumab Biorecognition on Agreement with ELISA

Mohammed N. Alabbasi[1]*, Amer Th. Al-Taee[2], Luay A. Al-Helaly[2]

[1]Department of Chemistry, College of Education for Women, University of Mosul, Mosul, Iraq
[2]Department of Chemistry, College of Science, University of Mosul, Mosul, Iraq
*Corresponding author: Mohammed Nayef Alabbasi
E-mail: mohammed.nayef@uomosul.edu.iq; Tel.: +964 77 08250825

ABSTRACT: A biosensor intended for serum measurement must be assessed against a comparator on the same specimens, because calibration behavior in buffer cannot establish agreement in a complex clinical matrix. This study compared nine label-free electrochemical immunosensors for serum human epidermal growth factor receptor 2 extracellular domain (HER2-ECD) in a paired subgroup of 25 women: eight healthy controls and 17 patients with breast cancer. Three working-electrode architectures—activated glassy carbon (GCE), poly(p-anisidine)-modified GCE (GCE/PPA), and ammonium alginate–tungsten trioxide-coated GCE/PPA [GCE/PPA/(AmAlg–WO3)]—were each combined with trastuzumab (AbT), pertuzumab (AbP), or an equal-total-mass trastuzumab/pertuzumab mixture (AbTP). For every coded specimen, 10 µL of undiluted serum was incubated on the sensor disk for 30 min. The current change was calculated as ΔIserum = I0 − Iserum and converted with the inverse calibration equation specific to that sensor. Matched HER2 concentrations were obtained by sandwich ELISA. Agreement was evaluated with Lin's concordance correlation coefficient (CCC), Bland–Altman bias and 95% limits of agreement, mean absolute error (MAE), root mean square error (RMSE), Deming regression, and stratified analyses. Absolute errors were also compared by Friedman and Holm-corrected paired tests. GCE/PPA/(AmAlg–WO3)/AbTP showed the strongest descriptive balance: CCC 0.926 (95% CI, 0.678–0.970), bias −6.16 ng mL−1, MAE 9.12 ng mL−1, and RMSE 12.14 ng mL−1. GCE/PPA/(AmAlg–WO3)/AbP was close (CCC 0.917; MAE 10.03 ng mL−1). Bare-GCE configurations tended toward positive bias, whereas PPA-containing configurations tended toward negative bias. Most Friedman comparison families were not significant; the only Holm-corrected pairwise difference involved AbP versus AbTP within GCE/PPA. The nanocomposite mixed-antibody configuration is therefore a promising candidate, but the small paired sample, broad confidence intervals, and nontrivial limits of agreement do not support interchangeability with ELISA or general statistical superiority.

1. INTRODUCTION

The extracellular domain of human epidermal growth factor receptor 2 (HER2-ECD) can be released into the circulation and measured in serum. Its analytical meaning differs from tissue HER2 assessment: serum HER2-ECD reflects a soluble receptor fragment, whereas immunohistochemistry and in situ hybridization characterize tumor tissue and remain central to therapeutic

classification. In some cases of monitoring, serum HER2-ECD could add complementary information, but its utility as a stand-alone diagnostic test is limited by several factors including variability in shedding, tumor volume, treatment regimens employed, and assay methodology [1–3]..

Electrochemical immunosensing presents a very convenient method for protein determination because of the conversion of antibody recognition into measurable changes in the current, potential, impedance, or transfer of interfacial charge. HER2 detecting systems described in scientific publications can be found in several formats including label-free, sandwich, nanolabel, hydrogel, and signal-amplified ones. However, since the matrix type and electrode material, as well as the antibody system configuration and the calibration method applied differ within various methods, the comparison of the measuring ranges and detection levels is not justified. Evidence obtained with recombinant protein in buffer or with spiked serum is especially distinct from evidence obtained in coded patient specimens measured against an established laboratory assay [4–6].

The present sensor system contains two design variables. Initially, there is electrode architecture: bare GCE that is activated, GCE with PPA coating, or GCE/PPA that has an AmAlg–WO_3 coating. Following that, there is biorecognition. The difference here is that, while trastuzumab fancy the HE2 domain IV, pertuzumab prefers domain II. Testing these two antibodies separately and with mass equal mixture should be used for reviewing the role of epitope selection without increasing total antibody mass of the mixture [7–8]. The question in question is which mixture provides a maximum signal, along with serum concentrations that are but close to an independent result obtained for the same samples.

This consideration necessitates the use of agreement analysis instead of just correlation. Two methods may move in the same direction while having respective bias either constant or proportional along with significant variations referring to the separate samples. Current instructions for comparing methods thus advise using pairs of samples covering the concentration range of interest with respect to bias assessment, agreement limits, regression behavior and accuracy measurement as well as correlation indices [9].

In this study, all nine immunosensors were assessed concerning the same set of 25 coded serum samples, thereby directly comparing each estimate with matching HER2-ELISA data. The study aimed at producing estimates about the role of electrode architecture and trastuzumab/pertuzumab recognition in (i) overall concordance, bias, and absolute error, (ii) patterns of agreement among healthy controls and patients, and (iii) rankings of paired absolute errors. The authors excluded results pertaining to calibration-development and wider clinical chemistry issues to keep the issue of serum method agreement at the center of the study.

2. MATERIALS AND METHODS

2.1 Paired-serum design and ethical conduct

In the paired analysis, 25 samples were chosen from the thesis cohort, namely, eight healthy individuals and 17 breast cancer patients. All the nine types of electrochemical immunosensors and HER2 ELISA were applied to each sample. This subgroup is not an independent cohort, because it was a small sample of common specimens that allowed in-specimen comparisons to be performed on all 3 × 3 electrochemical sensors. The samples were collected in cooperation with Mosul Specialty Oncology and Nuclear Medicine Hospital and Central Blood Bank of Mosul. The voltammetric studies were conducted in Department of Chemistry, College of Sciences, Mosul University, and immunological tests were done at external accredited laboratories.

Adult female participants became eligible once all urine and blood samples had been collected, along with the necessary data for coded linkage of samples. Breast cancer status was established from medical records, as women with a history of breast cancer diagnosis were ruled out as controls. Samples that were contaminated, severely hemolyzed, or untraceable were excluded from the study. This work was carried out only after obtaining necessary approvals from institutional, health, and ethical authorities, including Ministry of Health research project approval No. 01/2021. Informed consent was obtained from all respondents and sample codes were used in the analysis instead of personal identifiers.

2.2 Serum collection, storage, and coded linkage

Venous blood was collected using sterile materials and allowed to coagulate prior to centrifugation. The isolated serum was moved into clean coded containers and further split into appropriate aliquots where applicable in order to limit the number of freeze-thaw cycles. The samples were kept at 2-8 °C for timely analysis or at a temperature of -80 °C or lower for future testing.

Natural Resources for Human Health
eISSN: 2583-1194

Before testing, one of the aliquots was taken out and allowed to thaw gradually at room temperature and gently mixed without excessive shaking and foaming. The same code was maintained in the process of the electrochemical and ELISA measurement, enabling sample identification at the individual level without disclosing any identity information in the records.

2.3 Immunosensor configurations and sensor-specific calibration

Three different working-electrode configurations were applied, which were the activated glassy carbon electrode (GCE), the GCE that was electropolymerized using polypyrrole acid (PPA), and GCE/PPA that was covered with an AmAlg-WO_3 suspension. The activated surfaces were treated by EDC/NHS chemistry before being coated by trastuzumab (Ab_T) or pertuzumab (Ab_P), or a combination of both these two antibodies (Ab_{TP}) and then blocked using BSA. The single antibody systems used 0.50 µg of antibodies. The combination of the two antibodies was 0.25 µg of trastuzumab and 0.25 µg of pertuzumab, separated by the total amount of 0.50 µg of And thus the combinations produced GCE/Ab_T, GCE/Ab_P, GCE/Ab_{TP}, GCE/PPA/Ab_T, GCE/PPA/Ab_P, GCE/PPA/Ab_{TP}, GCE/PPA/(AmAlg–WO_3)/Ab_T, GCE/PPA/(AmAlg–WO_3)/Ab_P, and GCE/PPA/(AmAlg–WO_3)/Ab_{TP}.

Every installation has its own separate HER2-ECD calibration and differential-pulse-voltammetry method file. Serum responses were never calculated using the equation of another sensor. The calibration was determined with the baseline-adjusted saturation model, and its inverse variant was used to determine concentration. Only the model and the coefficients described in the thesis were used; no recalibration or an external experimental value has been incorporated in this analysis.

2.4 Measurement of undiluted serum by differential pulse voltammetry

Once the first current I_0 was measured, the immunosensor was taken from the electrochemical cell and moved into a vertical position such that the side with the working disk was turned upward. A sample of serum (10 µL) was delivered to the working surface in its original form and left for incubation for half an hour in a moisture chamber. The working disk was washed with phosphate-buffered saline and returned to the electrochemical cell showing its working surface downward, while the subsequent measurement was conducted. In this pair of samples, no serum dilution adjustment was applied.

$$\Delta I_{serum} = I_0 - I_{serum} \quad (1)$$

The resulting current change was transformed to the native serum HER2-ECD concentration with the sensor-specific inverse equation:

$$C = IC_{50,app} \times (\Delta I_{serum} - \Delta I_{blank})/(\Delta I_{blank} + \Delta I_{max} - \Delta I_{serum}) \quad (2)$$

Here, ΔI_{blank}, ΔI_{max}, and $IC_{50,app}$ are fitted parameters from that configuration's nonlinear calibration. Concentration estimates were reported in ng mL^{-1}. This calculation preserves the architecture-specific response relation and prevents apparent between-sensor differences from being obscured by a shared conversion equation.

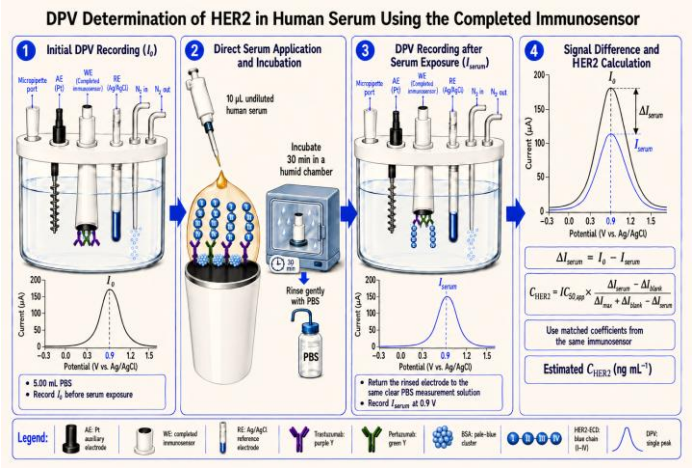

Figure 1. Determination of HER2-ECD in undiluted human serum by 10 µL disk incubation, PBS washing, DPV recording, and sensor-specific inverse calibration.

Natural Resources for Human Health
eISSN: 2583-1194

2.5 HER2 determination by ELISA

Matched HER2 concentrations were determined with the Solarbio Human CD340/ERBB2/HER2 ELISA kit (SEKH-0519), a sandwich enzyme immunoassay with a declared sensitivity of 23 pg mL^{-1}. BioTek TS 50 and TS 800 instruments were used for plate washing and absorbance measurement, respectively. Each run contained a complete standard series of 0, 46.87, 93.75, 187.5, 375, 750, 1500, and 3000 pg mL^{-1}. Standards, controls, and 100 µL serum specimens were loaded according to the kit procedure.

The plate was incubated for 120 min at 25 ± 2 °C with agitation, washed four times, and incubated for 60 min with diluted HRP-conjugated detection antibody. After a further four washes, TMB substrate was added and developed in the dark for 5–30 min. The reaction was stopped, and absorbance was read within 5 min at 450 nm with a 630 nm reference. Corrected absorbance was blank-adjusted and fitted with a four-parameter logistic model. Samples above the assay range were remeasured after dilution; direct extrapolation outside the calibration range was not accepted. Final concentrations were converted from pg mL^{-1} to ng mL^{-1}.

2.6 Pairing and statistical analysis

The unique specimen code was used to link electrochemical with ELISA data of the nine sensor configurations which were analyzed by means of Lin's CCC with 95% CI. In addition, the mean bias and LOA were calculated using Bland-Altman method, being HER2-DPV minus HER2-ELISA for the mean bias value. The average and squared error magnitudes were analyzed by MAE and RMSE. The method for detection of constant and proportional biases was Deming regression analysis where an intercept near 0 and slope near 1 were considered good descriptive parameters. The variable of Spearman correlation was used without interpretation of it as a proof of agreement when analysing separately the stratified groups.

Metrics were computed for all 25 paired samples first and then descriptively for eight controls and 17 patients. Since CCC is dependent on some existing variation of concentration across subjects, the control data are taken together with bias, MAE, and RMSE. It was predicted that the narrow concentration range and low n would produce unstable results even in cases with small absolute error.

In order to understand if the type of biorecognition or architecture impacted absolute error for the same samples, author investigated the issue in two ways through application of the Friedman test. At first, Friedman test was used in order to compare various biorecognition methods while keeping type of working electrode fixed. Then, second Friedman test was utilized in order to compare various types of working electrodes while keeping type of biorecognition the same. To compute the overall effect size Kendall's W was used. In instances where pairwise comparison was necessary the authors analyzed the data through Wilcoxon signed-rank test together with Hodges–Lehmann and rank-biserial correlation (r_{rb}).

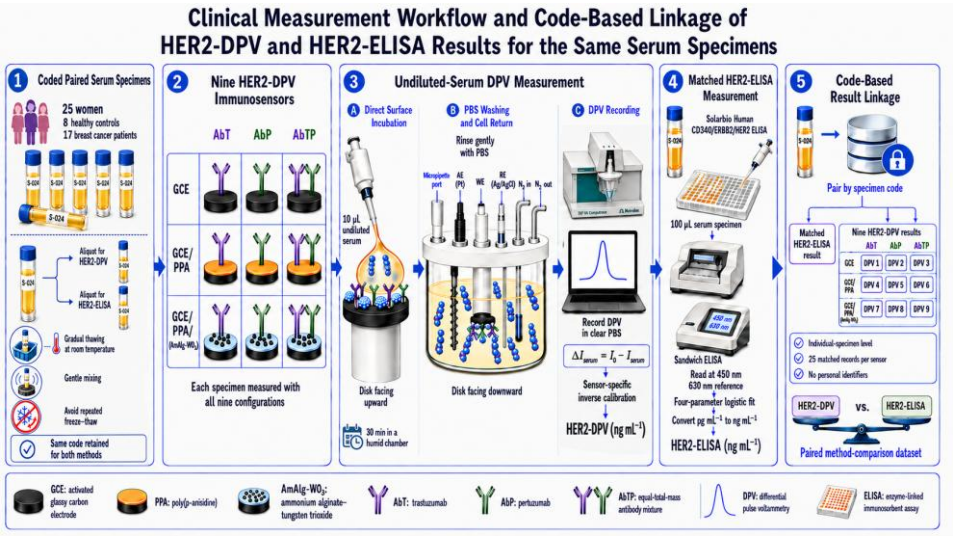

Figure 2. Clinical measurement workflow and code-based linkage of HER2-DPV and HER2-ELISA results for the same serum specimens.

Natural Resources for Human Health
eISSN: 2583-1194

3. RESULTS

3.1 Serum HER2 estimates across the nine configurations

The patients' estimates were above the controls for each sensor configuration. However, the levels differed according to the electrode and calibration equation to be employed. The bare-GCE systems provided the highest mean controls (12.35 -19.75 ng mL^{-1}) and patient amount (52.14 -54.37 ng mL^{-1}). The systems with PPA produced lower means, while the nanocomposite systems presented control means of 4.38 -7.71 ng mL^{-1} and patient means of 30.47 -34.86 ng mL^{-1}. This architectural effect happens in the case when samples are the same; thus, it represents the method effect rather than the biological sample changes.

Table 1. HER2-DPV estimates in the paired subgroup.

Configuration	Controls (n = 8), mean ± SD	Patients (n = 17), mean ± SD	Holm-adjusted p
GCE/Ab_T	19.75 ± 15.94	52.59 ± 40.24	.019
GCE/Ab_P	12.35 ± 7.71	52.14 ± 35.36	<.001
GCE/Ab_{TP}	12.86 ± 7.50	54.37 ± 37.81	<.001
GCE/PPA/Ab_T	6.57 ± 3.48	27.52 ± 21.57	<.001
GCE/PPA/Ab_P	5.59 ± 3.63	25.51 ± 20.54	<.001
GCE/PPA/Ab_{TP}	5.81 ± 3.79	30.88 ± 31.09	<.001
GCE/PPA/(AmAlg–WO_3)/Ab_T	4.95 ± 2.26	30.47 ± 23.14	<.001
GCE/PPA/(AmAlg–WO_3)/Ab_P	7.71 ± 7.07	34.13 ± 34.23	.019
GCE/PPA/(AmAlg–WO_3)/Ab_{TP}	4.38 ± 2.33	34.86 ± 35.57	<.001

Note. *Concentrations are ng mL^{-1}. Adjusted p values compare the patient and control distributions for each configuration. These group contrasts describe the paired subgroup and are not presented as diagnostic-performance estimates.*

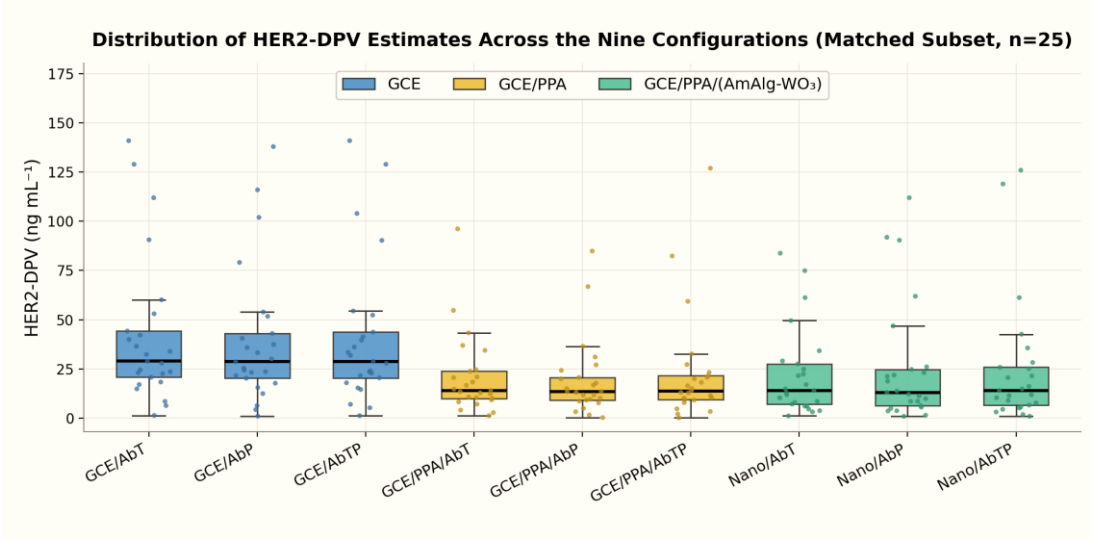

Figure 3. Distribution of HER2-DPV concentration estimates across the nine immunosensor configurations in the paired subgroup.

Within-sample trajectories were not parallel across the three electrodes. Some specimens showed only modest changes, whereas high-concentration specimens produced larger divergence after conversion from current to concentration. The same raw

Natural Resources for Human Health
eISSN: 2583-1194

specimen can therefore yield different concentration estimates when the response capacity and apparent half-saturation parameter differ between calibrations.

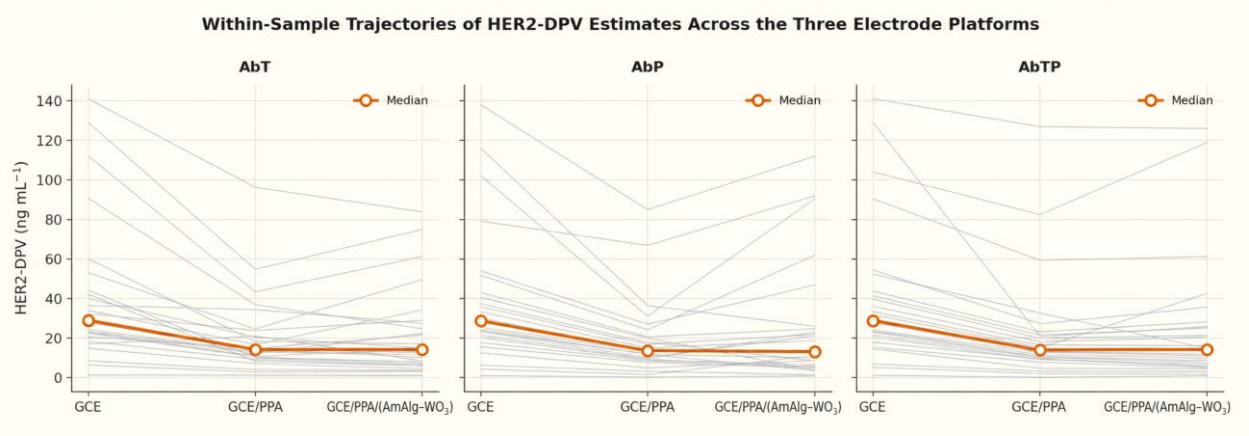

Figure 4. Within-specimen trajectories of HER2-DPV estimates across GCE, GCE/PPA, and GCE/PPA/(AmAlg–WO_3) for each biorecognition system.

3.2 Overall agreement with HER2-ELISA

The nine configurations differed in concordance, bias direction, and error. The three bare-GCE systems overestimated ELISA on average, with biases from +8.14 to +10.81 ng mL^{-1}. All PPA and nanocomposite systems underestimated ELISA on average, with biases from −5.59 to −12.13 ng mL^{-1}. Thus, adding PPA changed not only response magnitude but also the direction of average method difference in this paired dataset.

Table 2. Agreement between HER2-DPV and matched HER2-ELISA in all 25 paired samples.

Configuration	CCC [95% CI]	Bias	95% limits	MAE [95% CI]	RMSE [95% CI]	Deming intercept; slope
GCE/Ab_T	.815 [.391–.921]	10.81	[−25.21, 46.84]	15.59 [10.53–21.51]	21.01 [13.86–28.41]	3.07; 1.248
GCE/Ab_P	.757 [.359–.942]	8.14	[−34.59, 50.88]	12.96 [6.95–21.65]	22.86 [9.47–36.17]	2.94; 1.166
GCE/Ab_{TP}	.807 [.506–.948]	9.82	[−27.83, 47.47]	12.84 [7.53–20.02]	21.23 [10.40–32.36]	2.51; 1.234
GCE/PPA/Ab_T	.779 [.597–.905]	−10.45	[−39.22, 18.33]	12.43 [7.89–17.95]	17.78 [10.25–24.87]	0.92; 0.636
GCE/PPA/Ab_P	.722 [.379–.852]	−12.13	[−43.86, 19.60]	14.37 [9.14–20.06]	19.97 [12.69–26.57]	0.50; 0.596
GCE/PPA/Ab_{TP}	.870 [.484–.943]	−8.41	[−33.57, 16.75]	11.59 [8.04–15.65]	15.13 [10.83–19.24]	−5.42; 0.905
GCE/PPA/(AmAlg–WO_3)/Ab_T	.861 [.706–.908]	−8.96	[−31.52, 13.60]	10.25 [6.43–14.26]	14.40 [9.07–18.81]	−0.20; 0.720
GCE/PPA/(AmAlg–WO_3)/Ab_P	.917 [.677–.962]	−5.59	[−27.82, 16.64]	10.03 [7.24–12.90]	12.44 [9.45–15.07]	−5.67; 1.003

Natural Resources for Human Health
eISSN: 2583-1194

Configuration	CCC [95% CI]	Bias	95% limits	MAE [95% CI]	RMSE [95% CI]	Deming intercept; slope
GCE/PPA/(AmAlg–WO_3)/Ab_{TP}	.926 [.678–.970]	−6.16	[−27.08, 14.77]	9.12 [6.08–12.38]	12.14 [8.19–15.80]	−7.97; 1.058

Note. *Bias, limits of agreement, MAE, and RMSE are in ng mL^{-1}. Bias = HER2-DPV − HER2-ELISA. A CCC closer to 1, smaller error, intercept closer to 0, and slope closer to 1 indicate better descriptive agreement; no single metric establishes interchangeability.*

The best combined descriptive result was obtained with GCE/PPA/(AmAlg–WO_3)/Ab_{TP}: CCC 0.926, MAE 9.12 ng mL^{-1}, RMSE 12.14 ng mL^{-1}, and bias −6.16 ng mL^{-1}. GCE/PPA/(AmAlg–WO_3)/Ab_P was close, with CCC 0.917, MAE 10.03 ng mL^{-1}, RMSE 12.44 ng mL^{-1}, and bias −5.59 ng mL^{-1}. Its Deming slope was 1.003, the closest to unity, although the intercept was −5.67 ng mL^{-1}. The mixed-antibody nanocomposite system had a slope of 1.058 and intercept of −7.97 ng mL^{-1}. These values indicate favorable tracking over the observed range with a persistent negative offset.

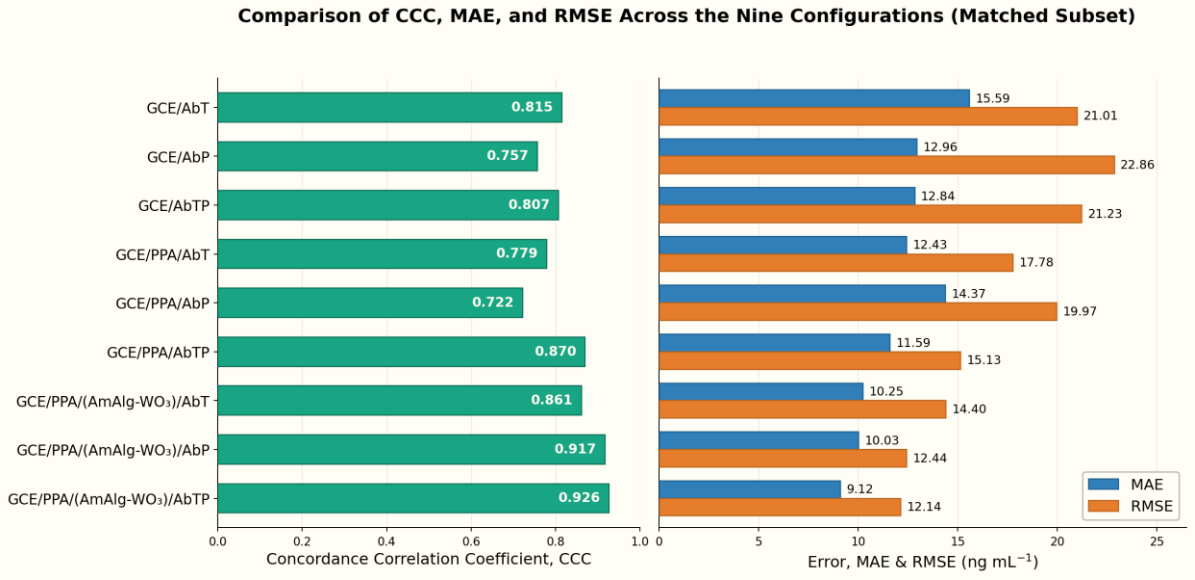

Figure 5. Comparative CCC, MAE, and RMSE profiles of the nine immunosensor configurations against matched HER2-ELISA.

3.3 Agreement within controls and patients

The CCC control results were quite low, ranging from only 0.099 to 0.310, yet this cannot be taken to suggest that there are no large absolute errors. The three PPA systems had controls with MAEs of 3.40–3.53 ng mL^{-1} whereas the nanocomposite Ab_T and Ab_{TP} systems had MAEs of 2.54 and 2.77 ng mL^{-1}, respectively. The low concordance coefficients reflect the combination of eight observations and limited between-control concentration variation. Among patients, nanocomposite Ab_P and Ab_{TP} gave the strongest concordance (0.903 and 0.904) and lowest MAEs (12.44 and 12.10 ng mL^{-1}) within that stratum.

Table 3. Group-stratified agreement and error.

Configuration	Control CCC	Control bias	Control MAE	Control RMSE	Patient CCC	Patient bias	Patient MAE	Patient RMSE
GCE/Ab_T	.127	13.75	14.19	19.26	.812	9.43	16.24	21.78
GCE/Ab_P	.111	6.35	7.43	9.57	.664	8.99	15.56	26.94

Configuration	Control CCC	Control bias	Control MAE	Control RMSE	Patient CCC	Patient bias	Patient MAE	Patient RMSE
GCE/Ab_{TP}	.099	6.86	7.61	9.82	.741	11.21	15.30	24.85
GCE/PPA/Ab_{T}	.228	0.57	3.49	4.03	.716	−15.63	16.63	21.38
GCE/PPA/Ab_{P}	.249	−0.41	3.40	4.04	.646	−17.64	19.53	24.05
GCE/PPA/Ab_{TP}	.236	−0.19	3.53	4.16	.836	−12.27	15.38	18.12
GCE/PPA/(AmAlg–WO_3)/Ab_{T}	.310	−1.05	2.54	3.29	.812	−12.68	13.87	17.32
GCE/PPA/(AmAlg–WO_3)/Ab_{P}	.217	1.71	4.93	6.68	.903	−9.02	12.44	14.37
GCE/PPA/(AmAlg–WO_3)/Ab_{TP}	.203	−1.62	2.77	3.74	.904	−8.29	12.10	14.50

Note. *Bias, MAE, and RMSE are in ng mL^{-1}. Control n = 8; patient n = 17. Confidence intervals and Spearman coefficients are available in the thesis source table. Because of the small control group and compressed range, control CCC should not be interpreted without the absolute-error measures.*

3.4 Paired absolute-error comparisons

Across all 25 specimens, MAE decreased from 15.59 ng mL^{-1} for GCE/Ab_T to 9.12 ng mL^{-1} for GCE/PPA/(AmAlg–WO_3)/Ab_{TP}. This descriptive gradient did not translate into a general omnibus difference. None of the six Friedman families was significant in the complete paired set. Within patients, only the comparison of recognition systems on GCE/PPA reached the omnibus threshold ($\chi^2 = 7.41$, $p = .025$; Kendall W = .218). All three architecture comparisons at fixed antibody system and the GCE and nanocomposite recognition-system families remained nonsignificant.

Table 4. Friedman tests of paired absolute error.

Scope	Comparison family	χ^2_F	p	Kendall W
All 25	Architecture within Ab_T	0.56	.756	.011
All 25	Architecture within Ab_P	2.88	.237	.058
All 25	Architecture within Ab_{TP}	0.96	.619	.019
All 25	Recognition system within GCE	5.36	.069	.107
All 25	Recognition system within GCE/PPA	3.84	.147	.077
All 25	Recognition system within nanocomposite	1.52	.468	.030
Patients 17	Architecture within Ab_T	1.06	.589	.031
Patients 17	Architecture within Ab_P	4.24	.120	.125
Patients 17	Architecture within Ab_{TP}	1.41	.494	.042
Patients 17	Recognition system within GCE	2.94	.230	.087
Patients 17	Recognition system within GCE/PPA	7.41	.025	.218
Patients 17	Recognition system within nanocomposite	0.82	.662	.024

Natural Resources for Human Health
eISSN: 2583-1194

Note. *Each family contains three repeated measurements on the same specimens. The complete control-only results were nonsignificant and are provided in the suggested supplementary material.*

Table 5. Holm-significant paired absolute-error comparisons.

Scope	Comparison	Median difference	Hodges–Lehmann	r_{rb}	Holm q
All 25	GCE/PPA/Ab_P − GCE/PPA/Ab_{TP}	0.24	0.72	.588	.026
Patients 17	GCE/PPA/Ab_P − GCE/PPA/Ab_{TP}	1.32	1.34	.830	.004

Note. *Differences are in absolute error (ng mL^{-1}). Positive values indicate larger absolute error for Ab_P than Ab_{TP} within the GCE/PPA architecture.*

The only retained pairwise result favored Ab_{TP} over Ab_P within GCE/PPA. In all 25 samples, the Hodges–Lehmann difference was 0.72 ng mL^{-1} (Holm q = .026; r_{rb} = .588); within patients it was 1.34 ng mL^{-1} (q = .004; r_{rb} = .830). No significant pairwise result established a general advantage of the nanocomposite architecture despite its lower descriptive errors.

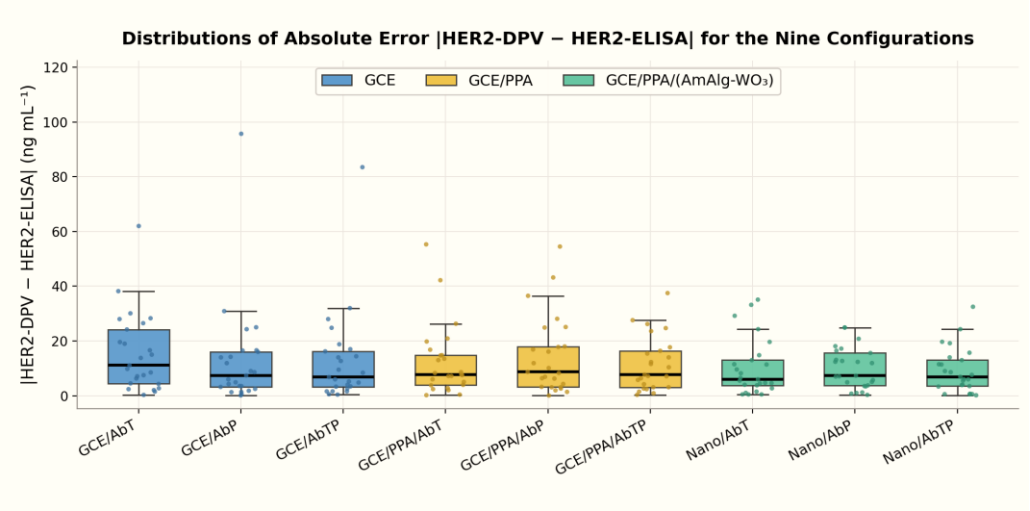

Figure 6. Distribution of absolute errors |HER2-DPV − HER2-ELISA| for the nine immunosensor configurations.

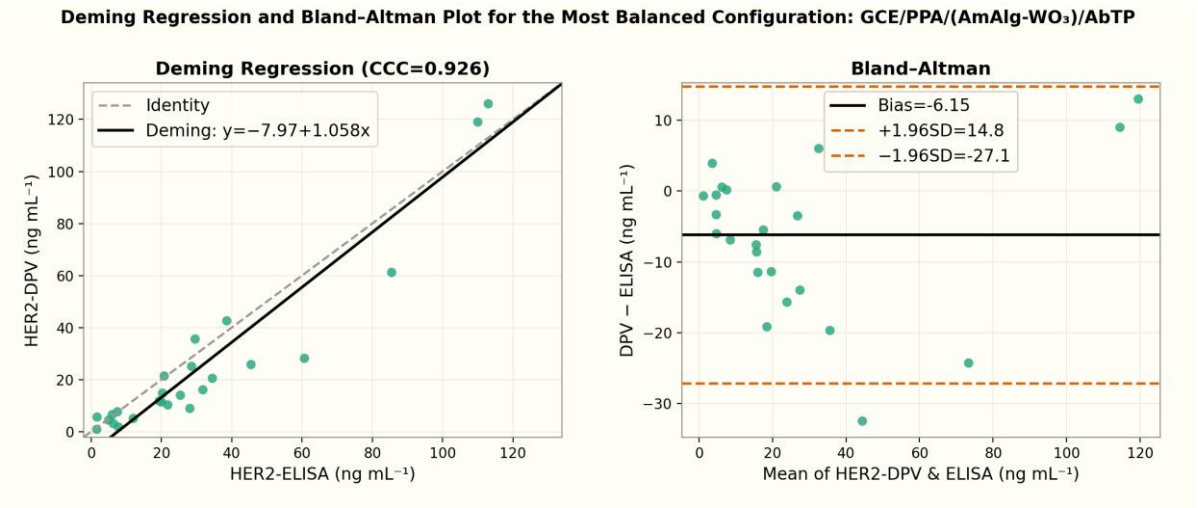

Figure 7. Deming regression and Bland–Altman plot for GCE/PPA/(AmAlg–WO_3)/Ab_{TP}, the configuration with the most balanced descriptive agreement.

Natural Resources for Human Health

eISSN: 2583-1194

4. DISCUSSION

4.1 The nanocomposite mixed-antibody sensor had the best descriptive balance

Observed result. GCE/PPA/(AmAlg–WO_3)/Ab_{TP} produced the highest overall CCC and the lowest MAE and RMSE among the nine sensors. Its average concentration was 6.16 ng mL^{-1} below ELISA, and the 95% limits of agreement extended from −27.08 to 14.77 ng mL^{-1}. The nanocomposite Ab_P system was close on every principal metric and had a Deming slope almost exactly equal to one.

Interpretation. The combined result suggests that the hydrated alginate–WO_3 layer and dual-epitope recognition generated a serum response that tracked the ELISA concentration range more consistently than the alternatives in this subset. This discovery is purely descriptive in nature and does not have a mechanistic basis; for example, the procedure failed to assess antifouling properties or the orientation of antibodies or the simultaneous occupancy of two antibodies or the roles of various serum interferences. Thus, nonzero negative bias demonstrates that improved agreement does not eradicate systematic disagreement.

Link to earlier work. The outcomes of electrochemical HER2 studies illustrated that matrix and interfacial design have a big impact on serum response in any type of hydrogel and label-free platforms [5–6]. The present data provide an internally controlled comparison between native, undiluted samples. However, they do not allow us to claim a clear numerical advantage over previously published sensors due to differences in sample preparation, assay type, reference method, and patient composition across different research papers.

4.2 Electrode architecture altered the direction of bias

The data collected indicate that the bare-GCE setups had a significant bias with respect to ELISA, while every PPA containing setup demonstrated the opposite trend. The transition took place in the cases of trastuzumab, pertuzumab, and the antibody cocktail, verifying an architecture-related trend rather than being specific for a single recognition element..

Interpretation. The concentration of serum was obtained using a sensor-specific nonlinear inverse equation, thus allowing for a change in concentration scale due to a surface that modifies signal accessibility, regardless of the raw currents showing similarities. The use of PPA can also impact the extent of nonspecific binding of proteins. However, the absence of direct quantification of these processes leads us to conclude that the architecture alters the bias of the empirical measurement method rather than naming a single physicochemical mechanism responsible for the process.

Relation to previous work. Modified electrodes are often evaluated through changes in peak current and analytical response. Work on indirect voltammetric determinations likewise demonstrates that an analyte-related interaction can be quantified through a change in another electrochemical feature rather than direct oxidation of the target [10–12]. In the current immunosensors, however, that functional signal had to be validated against the same serum target by ELISA; signal change alone could not establish concentration agreement.

4.3 The value of antibody mixing depended on the supporting surface

Observed result. Ab_{TP} did not improve every architecture uniformly. On GCE/PPA, it reduced MAE relative to Ab_P and was the only recognition comparison retained after Holm correction. On the nanocomposite surface, Ab_{TP} had the lowest descriptive error, but Ab_P was nearly equivalent. On bare GCE, Ab_P and Ab_{TP} had similar MAE, and the trastuzumab system had higher error in the 25-sample subset.

Interpretation. Distinct binding sites provide a rational reason to test a mixture, but surface immobilization can determine whether that complementarity is expressed analytically. The fact that total antibody mass was equal ruled out a simple explanation based on mass doubling. The findings suggest that there is some interaction between antibody composition and the surrounding environment. Since the binding density and orientation were not measured, this study cannot ascertain whether the mixed recognition resulted in increased number of epitopes available for recognition or interfaced only the block level.

Relation to previous work. Structural studies demonstrate that trastuzumab binds domain IV in HER2 while pertuzumab binds domain II [7–8]. Reviews on immobilization have contributed to the idea that epitope availability results from the type

of coupling chemistry as well as immobilization orientation on the transducer surface. Therefore, biologically complementary antibodies may not be analytically ideal on every electrode [13].

4.4 Agreement metrics answer different questions

Observed result. Although the best CCC values were greater than 0.90, it should be noted that the confidence intervals for the best values were wide, the mean biases were non-zero, and that the limits of agreement revealed differences that may be relevant to a single specimen. According to Deming regression, other fixed and proportional components were obtained: the slope of the nanocomposite Ab_P was 1.003; the intercept was -5.67 ng mL^{-1}; the slope of the mixed systems was 1.058 with the intercept of -7.97 ng mL^{-1}.

Interpretation. CCC is a combination of correlation and deviation from the identity line. MAE can be described as the summary of the average absolute difference. RMSE gives more importance to larger errors. Bland-Altman analysis is used for the representation of the distribution of paired differences. Deming regression is used to express fixed and proportional components. Favorable results in one of the methods can be compensated with unfavorable results obtained by other methods. The complete profile does not enable selection of candidates while enabling analytical interchangeability with ELISA.

Relation to previous work. Guidelines for method comparison advocate for the use of paired clinical specimens and an accurate evaluation of bias over the entire measurement range rather than only depending on correlation [9]. This is critical especially for serum HER2 as ELISA's performance is affected by calibration, specificity of the antibody, dilution, matrix composition, and therapeutic antibodies [14]. In this case ELISA was the comparator but not the error free definition of the true concentration.

4.5 Low control CCC did not imply uniformly poor low-range accuracy

The result being observed. The CCC values during the eight types of controls were always low for all types of sensors. However, in most of the cases, the PPA and nanocomposite systems had their MAE in controls less than 5 ng mL^{-1}. The nanocomposite Ab_T sensor added up to the largest control CCC, which was of 0.310, as well as the lowest MAE value of 2.54 ng mL^{-1}. However, the patient CCC values reached as high as 0.903–0.904 for the leading systems of nanocomposite technology..

Interpretation. When the range of the sample is narrowed, concordance becomes unstable. A small absolute difference may account for a large proportion of variation between individuals in controls, but a greater range of patients results in stronger assessments of rank and scale. Different strata allow the wide control–patient gap to not inflate the pooled association, however the eight-control estimates remain too inaccurate for detailed ranks.

Connection to earlier research. In prior research studies, the HER2-ECD serum studies show a large range of biological variability in patients and much less variability in controls [1,3]. Therefore, the present study interprets the statistical analysis of controls along with the MAE and bias, without assuming that low coefficients mean that all measurements obtained at low values were incorrect..

4.6 Paired tests restrained claims of superiority

Results observed. While the configurations of nanocomposite have three lowest total mean absolute error results, Friedman test does not indicate any significant architecture effects for an Ab_T, Ab_P or Ab_{TP}. The only significant omnibus family was observed for the antibody systems on GCE/PPA of the patients, where pairwise differences favored an Ab_{TP} when compared to an Ab_P.

Interpretation. The ranking arrives at a different conclusion than both the descriptive means used and the repeated-measures test. In the descriptive means, we can see that the correct candidate is determined, while the repeated measures test question whether the distribution of errors is stable across samples. With 25 samples, heterogeneous errors, and a large amount of concentration, the power of the measure decreases and its sensitivity to individual cases increases. Thus, the right conclusion is that GCE/PPA/(AmAlg–WO_3)/Ab_{TP} should be studied further, not shown universal superiority..

Relation to earlier research. Validation of clinical biosensors will be better when many samples, separate deliveries, and set basis for comparison are used rather than only taking the system from calibration limits [4,6]. Although the paired design applied is an important internal process, it is still less than what independent validation demands for clinical replacement..

4.7 Limitations

The main limit is the sample size: 25 samples were taken by all nine sensors, including eight controls. Therefore the confidence intervals were wide and subgroup estimates were sensitive due to the limited concentration range. The subgroup is a part of the cohort that enabled the thesis and there was no external validation of its results. An independent analysis by manufacturing batches was not carried out in the experiment, no predefined limits of reproducibility of lots were set and there was no second clinical comparator. Even though undiluted serum is a rigorous matrix for testing, specific interferents and recovery were not isolated in this comparison. Surface morphology, thickness (PPA), distribution of WO_3, orientation of the antibodies, antifouling conduct were not measured either. ELISA has its own limitations, there are problems with calibration and matrices, therefore it shouldn't be treated as a free-from-error method in this study.

5. CONCLUSIONS

Paired measurement of the same 25 serum specimens showed that both electrode architecture and antibody composition influenced agreement with HER2-ELISA. Bare-GCE sensors displayed positive mean bias, whereas PPA-containing sensors displayed negative mean bias. GCE/PPA/(AmAlg–WO_3)/Ab_{TP} provided the strongest descriptive balance of concordance and error, with CCC 0.926, MAE 9.12 ng mL^{-1}, RMSE 12.14 ng mL^{-1}, and bias −6.16 ng mL^{-1}; GCE/PPA/(AmAlg–WO_3)/Ab_P performed similarly. The paired tests did not demonstrate a general architecture advantage, and only the Ab_P-versus-Ab_{TP} comparison within GCE/PPA remained significant after Holm correction. The nanocomposite mixed-antibody configuration is therefore the leading candidate for larger evaluation, but its current limits of agreement and the uncertainty produced by the small internal subset preclude treating it as interchangeable with ELISA. Independent paired cohorts, between-batch reproducibility, interference testing, and predefined agreement criteria are required before clinical translation.

Data Scope

All experimental values, sample counts, equations, statistical results, and conclusions in this manuscript were taken exclusively from the paired human-serum and HER2-ELISA datasets of the doctoral thesis.

REFERENCES

[1] Perrier, A.; Gligorov, J.; Lefèvre, G.; Boissan, M. The extracellular domain of HER2 in serum as a biomarker of breast cancer. Laboratory Investigation 2018, 98, 696–707. https://doi.org/10.1038/s41374-018-0033-8

[2] Reix, N.; Malina, C.; Chenard, M.-P.; Bellocq, J.-P.; Delpous, S.; Molière, S.; Sevrin, A.; Neuberger, K.; Tomasetto, C.; Mathelin, C. A prospective study to assess the clinical utility of serum HER2 extracellular domain in breast cancer with HER2 overexpression. Breast Cancer Research and Treatment 2016, 160, 249–259. https://doi.org/10.1007/s10549-016-4000-z

[3] Shamshirian, A.; Aref, A.R.; Yip, G.W.; Ebrahimi Warkiani, M.; Heydari, K.; Razavi Bazaz, S.; Hamzehgardeshi, Z.; Shamshirian, D.; Moosazadeh, M.; Alizadeh-Navaei, R. Diagnostic value of serum HER2 levels in breast cancer: A systematic review and meta-analysis. BMC Cancer 2020, 20, 1049. https://doi.org/10.1186/s12885-020-07545-2

[4] Marques, R.C.B.; Viswanathan, S.; Nouws, H.P.A.; Delerue-Matos, C.; González-García, M.B. Electrochemical immunosensor for the analysis of the breast cancer biomarker HER2 ECD. Talanta 2014, 129, 594–599. https://doi.org/10.1016/j.talanta.2014.06.035

[5] Wang, W.; Han, R.; Chen, M.; Luo, X. Antifouling peptide hydrogel based electrochemical biosensors for highly sensitive detection of cancer biomarker HER2 in human serum. Analytical Chemistry 2021, 93, 7355–7361. https://doi.org/10.1021/acs.analchem.1c01350

[6] Wignarajah, S.; Chianella, I.; Tothill, I.E. Development of electrochemical immunosensors for HER-1 and HER-2 analysis in serum for breast cancer patients. Biosensors 2023, 13, 355. https://doi.org/10.3390/bios13030355

[7] Cho, H.-S.; Mason, K.; Ramyar, K.X.; Stanley, A.M.; Gabelli, S.B.; Denney, D.W., Jr.; Leahy, D.J. Structure of the extracellular region of HER2 alone and in complex with the Herceptin Fab. Nature 2003, 421, 756–760. https://doi.org/10.1038/nature01392

[8] Franklin, M.C.; Carey, K.D.; Vajdos, F.F.; Leahy, D.J.; de Vos, A.M.; Sliwkowski, M.X. Insights into ErbB signaling from the structure of the ErbB2–pertuzumab complex. Cancer Cell 2004, 5, 317–328. https://doi.org/10.1016/S1535-6108(04)00083-2

[9] Clinical and Laboratory Standards Institute. Measurement procedure comparison and bias estimation using patient samples, 3rd ed.; CLSI guideline EP09c; CLSI, 2018.

[10] Al-Hyali, R.H.; Al-Taee, A.T. Indirect determination of diclofenac sodium through its interaction with the aniline oxidation peak. Journal of the Turkish Chemical Society Section A: Chemistry 2024, 11, 47–54. https://doi.org/10.18596/jotcsa.1320484

[11] Al-Taee, A.T.; Al-Hafidh, A.Z. Indirect electrochemical determination of chlorpropamide through its interaction with valsartan using square wave voltammetry. Research Journal of Pharmacy and Technology 2021, 14, 6541–6544. https://doi.org/10.52711/0974-360X.2021.01131

[12] Alallaf, I.T.; Al-Taee, A.T.; Othman, N.S. Indirect electrochemical determination of carvedilol through its interaction with nitrous acid. Rafidain Journal of Science 2024, 33, 48–56. https://doi.org/10.33899/rjs.2024.183425

[13] Gao, S.; Guisan, J.M.; Rocha-Martin, J. Oriented immobilization of antibodies onto sensing platforms: A critical review. Analytica Chimica Acta 2022, 1189, 338907. https://doi.org/10.1016/j.aca.2021.338907

[14] Agnolon, V.; Contato, A.; Meneghello, A.; Tagliabue, E.; Toffoli, G.; Gion, M.; Polo, F.; Fabricio, A.S.C. ELISA assay employing epitope-specific monoclonal antibodies to quantify circulating HER2 with potential application in monitoring cancer patients undergoing therapy with trastuzumab. Scientific Reports 2020, 10, 3016. https://doi.org/10.1038/s41598-020-59630-y